Radiation Physics and Chemistry 107 (2015) 7–11

Contents lists available at ScienceDirect

Radiation Physics and Chemistry

journal homepage: www.elsevier.com/locate/radphyschem

Radiological characteristics of MRI-based VIP polymer gel under carbon beam irradiation

T. Maeyama [a,*], N. Fukunishi [a], K.L. Ishikawa [b,c], T. Furuta [d], K. Fukasaku [b,e], S. Takagi [b,f], S. Noda [b], R. Himeno [b], S. Fukuda [g]

[a] Nishina Center for Accelerator-Based Science, RIKEN, 2-1 Hirosawa, Saitama, Wako 351-0198, Japan
[b] Advanced Center for Computing and Communication, RIKEN, 2-1 Hirosawa, Saitama, Wako 351-0198, Japan
[c] Department of Nuclear Engineering and Management, Graduate School of Engineering, The University of Tokyo, 7-3-1 Hongo, Bunkyo, Tokyo 113-8656, Japan
[d] Nuclear Science and Engineering Center, Japan Atomic Energy Agency, 2-4 Shirakata-Shirane, Ibaraki, Tokai 319-1195, Japan
[e] Department of Neurosurgery, Himon'ya Hospital, 2-9-5 Minami, Meguro, Tokyo 152-0013, Japan
[f] Graduate School of Engineering, Department of Mechanical Engineering, The University of Tokyo, 7-3-1 Hongo, Bunkyo, Tokyo 113-8656, Japan
[g] Research Center for Charged Particle Therapy, National Institute of Radiological Sciences, 4-9-1 Anagawa, Inage, Chiba 263-8555, Japan

HIGHLIGHTS

- We study the radiological characteristics of VIP gel dosimeters under carbon beam irradiation.
- Linear energy transfer dependence was evaluated and discussed with simulation code PHITS.
- Contribution from secondly ion can explain results with different incident beam energy.

ARTICLE INFO

Article history:
Received 30 July 2014
Accepted 2 September 2014
Available online 8 September 2014

Keywords:
PHITS
Gel dosimeter
Dose-averaged LET
Three-dimensional dose distribution
LET dependence
Dose verification

ABSTRACT

We study the radiological characteristics of VIP polymer gel dosimeters under carbon beam irradiation with energy of 135 and 290 AMeV. To evaluate dose response of VIP polymer gels, the transverse (or spin–spin) relaxation rate R_2 of the dosimeters measured by magnetic resonance imaging (MRI) as a function of linear energy transfer (LET), rather than penetration depth, as is usually done in previous reports. LET is evaluated by use of the particle transport simulation code PHITS. Our results reveal that the dose response decreases with increasing dose-averaged LET and that the dose response–LET relation also varies with incident carbon beam energy. The latter can be explained by taking into account the contribution from fragmentation products.

© 2014 Elsevier Ltd. All rights reserved.

1. Introduction

Carbon-ion beams have a higher biological effectiveness and superior dose distribution than X-rays and gamma-rays, and have been established to have a therapeutic effect on solid cancers, and particularly radio-resistant cancers (Linz, 2012). In recent years, more sophisticated techniques have been developed, such as three-dimensional scanning irradiation, in which the aim is to avoid unnecessary damage to healthy tissue and to concentrate the dose on only tumor target (Minohara et al., 2010). Hence, it is increasingly important to develop dosimeters capable of simple and accurate measurement of three-dimensional dose distribution.

Polymer gel dosimeters (Baldock et al., 2010) consist of gel-fixed radiation-sensitive compounds that, upon irradiation, undergo polymerization as a function of absorbed dose. The three-dimensional (3D) dose distribution can be probed by magnetic resonance imaging (MRI) of the reaction products (Kennan et al., 1992; Maryanski et al., 1992). Gel dosimeters have been used for the verification of planned 3D dose distribution for the case of X-ray and gamma-ray radiotherapy (MacDougall et al., 2002; Vandecasteele and De Deene, 2013).

On the other hand, for heavy-ion beams, the sensitivity of virtually all kinds of gel dosimeters (except for recently developed nanocomposite Fricke gel (Maeyama et al., 2014a)) changes with radiation quality, which is determined by the charge and velocity of ions and cannot be evaluated directly from the obtained signal

* Corresponding author. Tel.: +81 48 467 9463; fax: +81 48 461 5301.
E-mail address: maeyama@riken.jp (T. Maeyama).

http://dx.doi.org/10.1016/j.radphyschem.2014.09.001
0969-806X/© 2014 Elsevier Ltd. All rights reserved.

strength (Baker et al., 2009; Kantemiris and et al., 2009; Ramm et al., 2004, 2000).

In this study, we evaluated the radiological characteristics of *N*-Vinylpyrrolidone based polymer gels (VIP gel) under carbon-ion beam irradiation. VIP gel, one of representative polymer gel dosimeters, was originally introduced by a Greek group in 1999 (Pappas et al., 1999). Its characterization and improvement have been reported in numerous investigations, especially for low LET radiation (Karaiskos et al., 2005; Kipouros et al., 2001; Kozicki et al., 2007; Pantelis et al., 2008; Papagiannis et al., 2001; Papoutsaki et al., 2013a, 2013b; Pappas et al., 2003, 2006, 2008, 2005, 2001). With its wide range of linear dose response up to ca. 40 Gy (Kipouros et al., 2001; Kozicki et al., 2007) and small dose rate dependence (Kipouros et al., 2001), VIP polymer gel is expected to be advantageous also for the case of high LET radiation. The distribution of the transverse relaxation rate R_2 in irradiated samples was measured by MRI. While the radiation sensitivity is usually plotted against penetration depth in most of existing study, we derive sensitivity calibration curves, more appropriately, as a function of linear energy transfer (LET). LET is a representative index of radiation quality and defined as the amount of energy transferred, per unit track length to the medium. Since LET is difficult to measure directly, we calculated it using the particle and heavy ion transport code system PHITS (Sato et al., 2013). Our results reveal that the response decreases with increasing dose-averaged LET and that the dose response–LET relation also varies with incident carbon beam energy. The latter can be explained by taking into account the contribution from fragmentation products.

2. Experimentation method

2.1. Irradiation

The irradiation experiments were conducted at two facilities: the Radioactive Isotope Beam Factory (RIBF) at the Institute of Physical and Chemical Research (RIKEN) and the Heavy Ion Medical Accelerator in Chiba (HIMAC) at the National Institute of Radiological Sciences (NIRS).

The experiment at RIBF was conducted using a carbon beam with 135 AMeV that was guided to E5B experimental vault. This carbon ion beam was spread laterally using a pair of wobbler magnets and a scatterer and had a uniform irradiation field with a diameter of approximately 8 cm and a controlled dose rate at the incident surface of about 10 Gy/min. A series of irradiation was conducted by using an automatic sample changer which automatically places each sample at the beam position (Ryuto et al., 2008). Irradiation experiments in the HIMAC-biology-beam port were conducted with a carbon beam (290 AMeV, 10 cm in diameter) spread laterally using a pair of wobbler magnets and a scatterer that had a dose rate at the incident surface of 10 Gy/min, similarly to the experiments at RIBF.

2.2. Gel dosimeter preparation

VIP gel dosimeters were prepared as reported in the literature (Kantemiris et al., 2009; Karaiskos et al., 2005; Kipouros et al., 2001; Pappas et al., 1999; Petrokokkinos et al., 2009). The VIP dosimeter was composed of 4% (w/v) *N*,*N*′-methylenebisacrylamide, 8% (w/v) *N*-vinyl-2-pyrrolidone, 7.5% (w/v) gelatin and a small amount of oxygen absorber (0.0008% (w/v) copper(II) sulfate, 0.007% (w/v) ascorbic acid). The prepared gel solution was sealed into PET containers and left to solidify for a day.

2.3. MRI analysis

MRI analysis of the gel dosimeters was conducted using a 1.5 T MRI scanner (Intera Achieva Nova Dual, Philips Medical Systems, Best, Netherlands). The MR relaxation time ($R_2 = 1/T_2$) was determined using a turbo mixed sequence (Denkleef and Cuppen, 1987). The analysis conditions were TR=3000 ms; TE=800 and 20 ms; TI=200 ms; ETL=86; pixel spacing=0.78 mm.

2.4. Measurement using ionization chamber

The dose at the same position as the sample was measured in advance by using a Markus ionization chamber. Based on the dose thus evaluated, the accumulated dose at the incident surface during sample irradiation can be determined by using a secondary electron monitor or another ionization chamber installed permanently on the upstream side of the beam line. The depth–dose distribution was measured as described in Kanai et al. (2004). The range shifters are made of aluminum at RIKEN (Ryuto et al., 2008) and PMMA at NIRS (Minohara et al., 2010). The smallest interval is determined by the thickness of the thinnest range shifters (24 μm aluminum at RIKEN, 500 μm PMMA at HIMAC). Also, the depth–dose distributions in the VIP gel were evaluated using them as range shifters with a minimal step size of 1 mm. Various combinations of rectangular acryl containers with thicknesses of 2, 5, 10 and 20 mm (up to two containers with each thickness) were used to vary the total thickness of the VIP gel.

2.5. PHITS calculation

PHITS is a three-dimensional general-purpose Monte Carlo code, and can deal with the transport of nearly all particles, including neutrons, protons, heavy ions, photons and electrons over wide energy ranges using various nuclear reaction models and data libraries (Sato et al., 2013). In our PHITS simulations, SPAR model was chosen for the calculations of LET (Armstrong and Chandler, 1973). In addition, the energy straggling and angular dispersion were included, and the event generator mode was used. To reduce the computation time, collimators, scatterers and wobblers were not explicitly considered, and the computation was conducted for the vicinity of the irradiated sample surface. The incident energy was taken as 127.4 AMeV (RIBF) and 287.4 AMeV (HIMAC) from the residual range of the carbon beam evaluated through ionization chamber measurements. These values are lower than the nominal extraction energy (135 and 290 AMeV) due to the energy loss during beam transportation to the incident surface, and consistent with those reported in the literature (Matsufuji et al., 2003; Ryuto et al., 2008) within the day-to-day variation. The elemental composition of VIP gel reported by Kantemiris et al. (2009) was used.

Let us denote the dose deposited by particles whose LET is between L and $L+dL$ as $D(L)dL$; the absorbed dose is given by $\int_0^\infty D(L)dL$. Using the functionality of the PHITS code, we tallied the LET-resolved dose or LET distribution $D(L)$ in terms of dose, dose-averaged LET (L_{ave}), and dose-averaged response (R_{ave}) at different penetration depths. L_{ave} and R_{ave} are defined as

$$L_{ave} = \frac{\int L\, D(L)dL}{\int D(L)dL}, \quad (1)$$

$$R_{ave} = \frac{\int R(L)D(L)dL}{\int D(L)dL}, \quad (2)$$

respectively.

3. Results and discussion

3.1. Dose and R_2 distribution

The depth–dose distribution and depth–R_2 distribution obtained at RIBF are shown in Fig. 1. Fig. 1(a) shows the depth–dose distribution obtained with the ionization chamber using different kinds of range shifters. The lines indicate the dose distributions calculated with PHITS. A comparison of the experimental and simulation results reveals close agreement, particularly with respect to the range (within 1 mm).

The R_2 distributions in VIP gel obtained through MRI measurements are shown in Fig. 1(b). The height of the Bragg peaks is reduced, compared with Fig. 1(a), since the gel response decreases with LET, which increases with depth, as discussed below. Nevertheless, the peak positions for different irradiation doses agree with each other within one pixel. Furthermore, they are consistent with the range obtained with the ionization chamber [Fig. 1(a)] within one pixel. Hence, the VIP gel can evaluate the range within 1–2 mm, though its LET-dependent response hinders direct evaluation of dose distribution.

3.2. LET dependence of dose response for VIP gels

Let us analyze the LET dependence of the dose response of VIP gels more quantitatively. The dependence of the R_2 value on the dose at the incident surface is plotted for several different depths in Fig. 2. The response was found to be linear at each depth. The dose responses for entrance surface dose were evaluated from the slope in the range of 0–20 Gy and shown in Fig. 3 with the physical dose distribution calculated by PHITS. The physical dose was scored with the same resolution in the depth direction as in the MRI analysis (0.78 mm). The peak enhancement of the R_2 distribution, defined as the ratio of peak height to the value at the incident surface, was 1.7, whereas that of the physical dose distribution was 6. Thus, the radiation detection sensitivity decreases to less than one-third at the peak position, due to the increase in LET.

One can see from Fig. 3 that the dose response for the $^{12}C^{6+}$ 290 AMeV beam (HIMAC) was higher than for the $^{12}C^{6+}$ 135 AMeV beam (RIBF) both at the incident surface and at the Bragg peaks. The dependence of the dose response on the dose-averaged LET

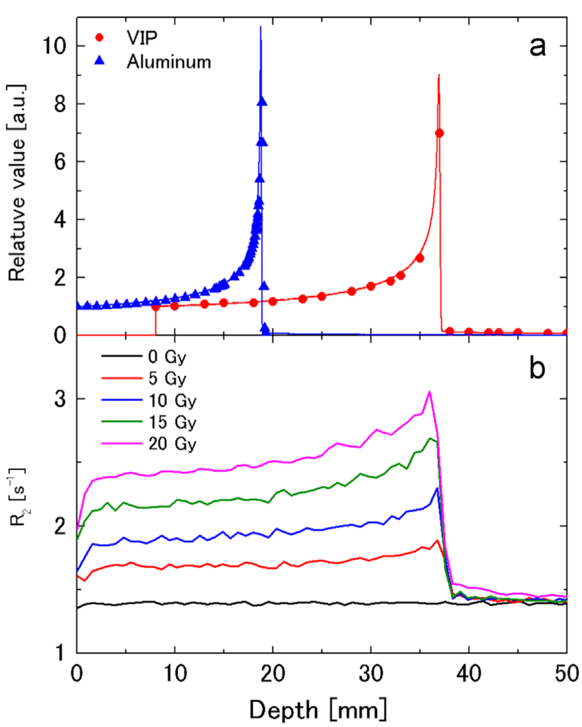

Fig. 1. Depth–dose distribution with 135-AMeV $^{12}C^{6+}$. (a) Distributions obtained with an ionization chamber using Al and VIP as range shifters. Symbols: measurements. Lines: PHITS calculation. (b) R_2 distribution of VIP gels measured by MRI (Maeyama et al., 2014b).

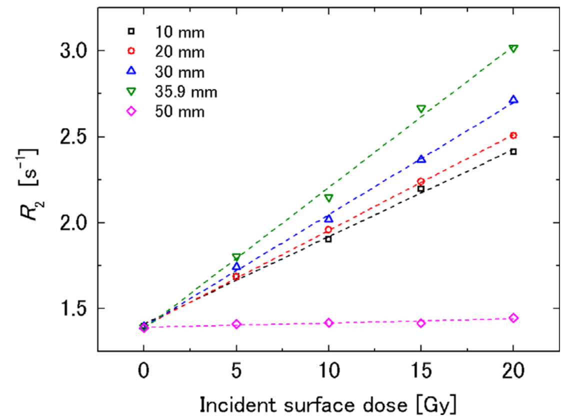

Fig. 2. R_2 in VIP gels vs. entrance surface dose at five different depths from the entrance surface.

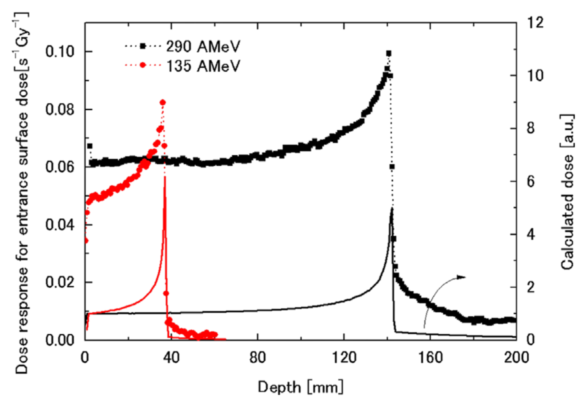

Fig. 3. Comparison between the dose response (symbols) and calculated dose distribution (solid lines) in the VIP gel with 135 and 290-AMeV $^{12}C^{6+}$ (Maeyama et al., 2014b).

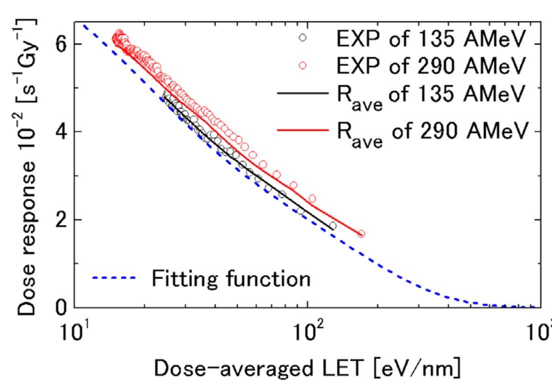

Fig. 4. Dose response of VIP gel for irradiation of 135 AMeV (squares) and 290 AMeV (circles) as a function of dose-averaged LET. The solid lines show dose-averaged response calculated from Eq. (2), and the dotted line shows the fitting curve from Eq. (3) as a function of mono-LET.

[Eq. (1)] is shown in Fig. 4. The dose response for the 290 AMeV beam is approximately 10% higher than for the 135 AMeV beam at the same dose-averaged LET.

The results in the previous paragraph indicate that the dose response of the gel is not uniquely determined by the dose-averaged LET but also by the details of the contribution from secondary ions generated in nuclear fragmentation reactions between the incident and target nuclei. The LET spectra of different particles for the 135 and 290 AMeV beams, calculated using the PHITS code, are plotted in Fig. 5 for the case of L_{ave}=47 [eV/nm]. ^{12}C forms a sharp peak at the same position irrespective of incident energy; more secondary ions

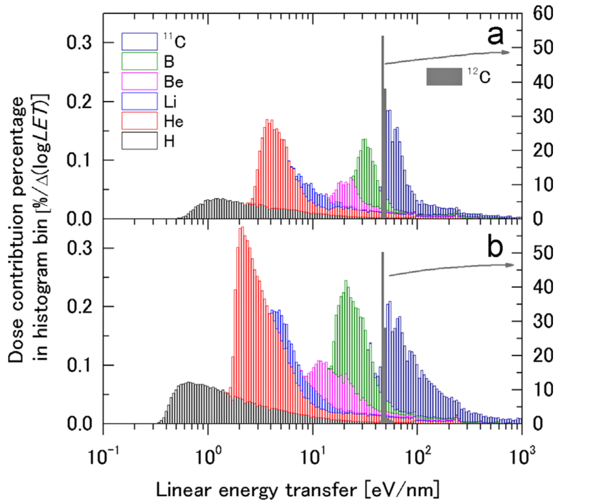

Fig. 5. LET distribution as a stacked histogram at the same dose-averaged LET (47 eV/nm) for 135 AMeV (a) and 290 AMeV (b). Open and solid bars correspond to secondary (left axis) and primary ions (right axis), respectively. Bin width Δ (log LET) = 0.054.

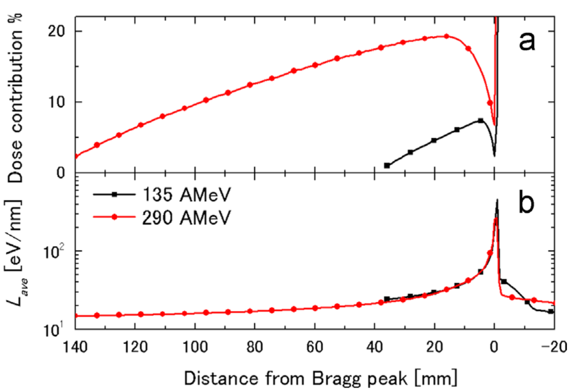

Fig. 6. (a) Relative contribution from secondary ions to dose and (b) dose-averaged LET for irradiation of 135-AMeV and 290-AMeV $^{12}C^{6+}$ as a function of the distance from the Bragg peak.

with broader LET distributions are produced for the case of the 290 AMeV beam. From Fig. 6(a), we can see that the contribution from the secondary ions to the dose strongly depends on the incident energy, while the curves for the dose-averaged LET in Fig. 6(b) closely overlap each other. The former increases with penetration depth and reaches a maximum of 7% and 19% at 135 and 290 AMeV incident energies, respectively [Fig. 6(a)]. Thus, secondary ions make a substantial contribution even in the case of the 135 AMeV beam.

The circles in Fig. 4 are plotted against the dose-averaged LET L_{ave} and depend on the incident energy, as we have discussed above. If we assume that the radiation detection sensitivity is a unique function $R(L)$ of the LET L of each projectile, independent of its species, we can express the response R_{ave} averaged over the LET distribution as Eq. (2).

Let us fit $R(L)$ with a function of the following form:

$$R(L) = a_1 * \exp\left(-\frac{L}{t_1}\right) + (a_0 - a_1) * \exp\left(-\frac{L}{t_2}\right) \quad (3)$$

The value of a_0, corresponding to the low LET limit, was set to the previously reported value of 0.09 s^{-1} Gy^{-1} (Petrokokkinos et al., 2009). Eq. (3) ensures the high LET limit of $\lim_{L=\infty} R(L) = 0$. The other parameters were determined as $a_1 = 0.0494$ s^{-1} Gy^{-1}, $t_1 = 17.74$ eV/nm, and $t_2 = 140.844$ eV/nm, through fitting the R_{ave}–L_{ave} relation calculated with Eqs. (1)–(3) and the LET distribution $D(L)$ as in Fig. 5 to the experimental values plotted in Fig. 4 with circles for the two incident energies. The obtained fitting function Eq. (3) is plotted as a dashed line in Fig. 4.

Thus calculated dose-averaged response at 135 and 290 AMeV is shown as lines in Fig. 4, which are in close agreement with the experimental results. The observation that a single response function Eq. (3) can reproduce the R_{ave}–L_{ave} relation for both incident energies strongly supports our speculation that the dependence on the incident energy found in Figs. 3 and 4 is due to the contribution from fragmentation products. Using Jensen's inequality (Jensen, 1906), one can show that the broader the LET distribution, the larger the dose-averaged response R_{ave}, if $R(L)$ is convex within the relevant range of LET. R_{ave} is slightly different from R even at the incident surface due to contribution from a small fraction (0.05% at 135 AMeV in terms of dose) of high-LET (~1000 eV/nm) target fragments such as N and O.

4. Conclusion

We investigated the LET-dependence of the sensitivity of VIP polymer gel dosimeters under carbon beam irradiation, using the measurements by an ionization chamber as a reference to the physical dose and the PHITS code as a complementary means to calculate the distribution of the dose and dose-averaged LET. Calibration curves (radiation sensitivity vs. dose-averaged LET) depend on the incident energy, due to larger contribution from fragmentation products for higher incident energy, which increases sensitivity in total.

Acknowledgment

This research has been carried out as a Research Project with Heavy Ions at NIRS-HIMAC. This research was supported by Research and Development of the Next-Generation Integrated Simulation of Living Matter, which is a part of the development and use of the Next-Generation Supercomputer Project of MEXT, Japan, as well as by RIKEN President's Discretionary Fund (Strategic Programs for R&D). TF and TM gratefully acknowledge support by the RIKEN Special Postdoctoral Researchers Program. TM also acknowledges support by The Grant-in-Aid for Young Scientists (B-16310036).

References

Armstrong, T.W., Chandler, K.C., 1973. (ORNL Report ORNL-4869). SPAR, a FORTRAN Program for Computing Stopping Powers and Ranges for Muons, Charged Pions, Protons,and Heavy Ions. ORNL, Oak Ridge, TN, USA.

Baker, C.R., Quine, T.E., Brunt, J.N.H., Kacperek, A., 2009. Monte Carlo simulation and polymer gel dosimetry of 60 MeV clinical proton beams for the treatment of ocular tumours. Appl. Radiat. Isot. 67, 402–405.

Baldock, C., De Deene, Y., Doran, S., Ibbott, G., Jirasek, A., Lepage, M., McAuley, K.B., Oldham, M., Schreiner, L.J., 2010. Polymer gel dosimetry. Phys. Med. Biol. 55, R1–R63.

Denkleef, J., Cuppen, J.J.M., 1987. RLSQ: T1, T2, and rho calculations, combining ratios and least squares. Magn. Reson. Med. 5, 513–524.

Jensen, J.L.W.V., 1906. Sur les fonctions convexes et les inégalités entre les valeurs moyennes. Acta Math. 30, 175–193.

Kanai, T., Fukumura, A., Kusano, Y., Shimbo, M., Nishio, T., 2004. Cross-calibration of ionization chambers in proton and carbon beams. Phys. Med. Biol. 49, 771–781.

Kantemiris, I., et al., 2009. Carbon beam dosimetry using VIP polymer gel and MRI. J. Phy.: Conf. Ser. 164, 012055.

Karaiskos, P., Petrokokkinos, L., Tatsis, E., Angelopoulos, A., Baras, P., Kozicki, M., Papagiannis, P., Rosiak, J.M., Sakelliou, L., Sandilos, P., Vlachos, L., 2005. Dose verification of single shot gamma knife applications using VIPAR polymer gel and MRI. Phys. Med. Biol. 50, 1235–1250.

Kennan, R.P., Maryanski, M.J., Zhong, J., Gore, J.C., 1992. Hydrodynamic effects and cross relaxation in cross linked polymer gels. In: Proceedings of the International Society for Magnetic Resonance in Medicine.

Kipouros, P., Pappas, E., Baras, P., Hatzipanayoti, D., Karaiskos, P., Sakelliou, L., Sandilos, P., Seimenis, I., 2001. Wide dynamic dose range of VIPAR polymer gel dosimetry. Phys. Med. Biol. 46, 2143–2159.

Kozicki, M., Maras, P., Rybka, K., Biegański, T., Kadłubowski, S., Petrokokkinos, L., 2007. On the development of the VIPAR polymer gel dosimeter for three-dimensional dose measurements. Macromol. Symp. 254, 345–352.

Linz, U., 2012. Ion Beam Therapy: Fundamentals, Technology, Clinical Applications. Springer, Berlin Heidelberg.

MacDougall, N., Pitchford, W.G., Smith, M.A., 2002. A systematic review of the precision and accuracy of dose measurements in photon radiotherapy using polymer and Fricke MRI gel dosimetry. Phys. Med. Biol. 47, R107–R121.

Maeyama, T., Fukunishi, N., Ishikawa, K.L., Furuta, T., Fukasaku, K., Takagi, S., Noda, S., Himeno, R., Fukuda, S., 2014a. A diffusion-free and linear-energy-transfer-independent nanocomposite Fricke gel dosimeter. Radiat. Phys. Chem. 96, 92–96.

Maeyama, T., Fukunishi, N., Ishikawa, K.L., Furuta, T., Fukasaku, K., Takagi, S., Noda, S., Himeno, R., Fukuda, S., 2014b. Linear energy transfer dependence of VIP polymer gel dosimeters under carbon beam irradiation. Housyasenkagaku 98, 11–15.

Maryanski, M.J., Gore, J.C., Schulz, R.J., 1992. 3-D radiation dosimetry by MRI: solvent proton relaxation enhancement by radiation-controlled polymerisation and cross-linking in gels. In: Proceedings of the International Society for Magnetic Resonance in Medicine.

Matsufuji, N., Fukumura, A., Komori, M., Kanai, T., Kohno, T., 2003. Influence of fragment reaction of relativistic heavy charged particles on heavy-ion radiotherapy. Phys. Med. Biol. 48, 1605–1623.

Minohara, S., Fukuda, S., Kanematsu, N., Takei, Y., Furukawa, T., Inaniwa, T., Matsufuji, N., Mori, S., Noda, K., 2010. Recent innovations in carbon-ion radiotherapy. J. Radiat. Res. 51, 385–392.

Pantelis, E., Antypas, C., Petrokokkinos, L., Karaiskos, P., Papagiannis, P., Kozicki, M., Georgiou, E., Sakelliou, L., Seimenis, I., 2008. Dosimetric characterization of CyberKnife radiosurgical photon beams using polymer gels. Med. Phys. 35, 2312–2320.

Papagiannis, P., Pappas, E., Kipouros, P., Angelopoulos, A., Sakelliou, L., Baras, P., Karaiskos, P., Seimenis, I., Sandilos, P., Baltas, D., 2001. Dosimetry close to an Ir-192 HDR source using N-vinylpyrrolidone based polymer gels and magnetic resonance imaging. Med. Phys. 28, 1416–1426.

Papoutsaki, M.-V., Pappas, E., Papadakis, A.E., Varveris, C., Damilakis, J., Maris, T.G., 2013a. Polymer gel dosimetry utilizing a 2D (SE) and a 2D (HASTE) multiple echo sequences. J. Phys.: Conf. Ser. 444, 012088.

Papoutsaki, M.V., Maris, T.G., Pappas, E., Papadakis, A.E., Damilakis, J., 2013b. Dosimetric characteristics of a new polymer gel and their dependence on post-preparation and post-irradiation time: effect on X-ray beam profile measurements. Phys. Med. 29, 453–460.

Pappas, E., Angelopoulos, A., Kipouros, P., Vlachos, L., Xenofos, S., Seimenis, I., 2003. Evaluation of the performance of VIPAR polymer gels using a variety of x-ray and electron beams. Phys. Med. Biol. 48, N65–N73.

Pappas, E., Maris, T., Angelopoulos, A., Paparigopoulou, M., Sakelliou, L., Sandilos, P., Voyiatzi, S., Vlachos, L., 1999. A new polymer gel for magnetic resonance imaging (MRI) radiation dosimetry. Phys. Med. Biol. 44, 2677–2684.

Pappas, E., Maris, T.G., Papadakis, A., Zacharopoulou, F., Damilakis, J., Papanikolaou, N., Gourtsoyiannis, N., 2006. Experimental determination of the effect of detector size on profile measurements in narrow photon beams. Med. Phys. 33, 3700–3710.

Pappas, E., Maris, T.G., Zacharopoulou, F., Papadakis, A., Manolopoulos, S., Green, S., Wojnecki, C., 2008. Small SRS photon field profile dosimetry performed using a PinPoint air ion chamber, a diamond detector, a novel silicon-diode array (DOSI), and polymer gel dosimetry. Analysis and intercomparison. Med. Phys. 35, 4640–4648.

Pappas, E., Petrokokkinos, L., Angelopoulos, A., Maris, T.G., Kozicki, M., Dalezios, I., Kouloulias, V., 2005. Relative output factor measurements of a 5 mm diameter radiosurgical photon beam using polymer gel dosimetry. Med. Phys. 32, 1513–1520.

Pappas, E., Seimenis, I., Angelopoulos, A., Georgolopoulou, P., Kamariotaki-Paparigopoulou, M., Maris, T., Sakelliou, L., Sandilos, P., Vlachos, L., 2001. Narrow stereotactic beam profile measurements using N-vinylpyrrolidone based polymer gels and magnetic resonance imaging. Phys. Med. Biol. 46, 783–797.

Petrokokkinos, L., Kozicki, M., Pantelis, E., Antypas, C., Fijuth, J., Karaiskos, P., Sakelliou, L., Seimenis, I., 2009. Characterization of a new polymer gel for radiosurgery dosimetry using Magnetic Resonance Imaging. J. Instrum.4, P06018.

Ramm, U., Moog, J., Spielberger, B., Bankamp, A., Botcher, H.D., Kraft, G., 2004. Investigations of dose response of BANG (R) polymer-gels to carbon ion irradiation. Radiother. Oncol. 73, S99–S101.

Ramm, U., Weber, U., Bock, M., Kramer, M., Bankamp, A., Damrau, M., Thilmann, C., Bottcher, H.D., Schad, L.R., Kraft, G., 2000. Three-dimensional BANG (TM) gel dosimetry in conformal carbon ion radiotherapy. Phys. Med. Biol. 45, N95–N102.

Ryuto, H., Fukunishi, N., Hayashi, Y., Ichida, H., Abe, T., Kase, M., Yano, Y., 2008. Heavy-ion beam irradiation facility for biological samples in RIKEN. Plant Biotechnol. 25, 119–122.

Sato, T., Niita, K., Matsuda, N., Hashimoto, S., Iwamoto, Y., Noda, S., Ogawa, T., Iwase, H., Nakashima, H., Fukahori, T., Okumura, K., Kai, T., Chiba, S., Furuta, T., Sihver, L., 2013. Particle and heavy ion transport code system, PHITS, version 2.52. J. Nucl. Sci. Technol. 50, 913–923.

Vandecasteele, J., De Deene, Y., 2013. On the validity of 3D polymer gel dosimetry: I. Reproducibility study. Phys. Med. Biol. 58, 19–42.